

# Unsteady Double Diffusive Mixed Convective Flow Over a Vertical Permeable Plate in a Porous Medium

Suresh Babu Ramakrishna <sup>1\*</sup>, Dinesh Pobbathy Aswathanarayana <sup>1</sup>, Nagalapura Lakshminarayana Ramesh <sup>1</sup>, Avula Sreevallabha Reddy <sup>1</sup>

<sup>1</sup> Department of Mathematics, Ramaiah Institute of Technology, Bangalore-54, India; sureshbabu\_r80@yahoo.co.in (S.B.R.); dineshpa@msrit.edu (D.P.A.); nlramesh1966@gmail.com (N.L.R.); sreensiri@gmail.com (A.S.R.);

\* Correspondence: sureshbabur\_r80@yahoo.co.in (S.B.R.);

Scopus Author ID 57199323358

Received: 1.12.2021; Accepted: 4.01.2022; Published: 12.02.2022

**Abstract:** In this article, we analytically investigated the effects of fluctuating free stream and suction velocities on unsteady mixed convective flow over a vertical permeable plate in the occurrence of an unvarying porous medium with a thin environment, time-dependent suction, and viscous dissipation. The governing equations of the physical phenomena give rise to a bunch of extremely non-linear coupled PDE's involving various non-dimensional parameters. An analytical solution has been obtained through the plots for distinct chief physical parameters like Grashof number, the amplitude of the fluctuating suction velocity parameter, amplitude of fluctuating free stream velocity parameter, Prandtl number, permeability parameter, solutal Grashof number, and Eckert number, which are involved in the solution. Also, a comparison has been made with published results in the absence of some non-dimensional parameters for a particular case and found in good agreement. The study results that the fluctuating free stream velocity increases the velocity, temperature increases, and a reverse tendency is observed in the Eckert number.

**Keywords:** Double diffusive; fluctuating flow; mixed convection; viscous dissipation; porous medium; perturbation technique.

© 2022 by the authors. This article is an open-access article distributed under the terms and conditions of the Creative Commons Attribution (CC BY) license (<https://creativecommons.org/licenses/by/4.0/>).

## Nomenclature:

|       |                                       |                      |   |
|-------|---------------------------------------|----------------------|---|
| $x$   | Distance along with the plate ( $m$ ) | $y$                  | Distance perpendicular to the plate ( $m$ )         |
| $p$   | Pressure                              | $ L $                | Amplitude of skin friction                          |
| $g$   | Gravitational force ( $m s^{-1}$ )    | $ Q $                | Amplitude of the heat flux                          |
| $t$   | Dimensional time ( $See$ )            | $\theta$             | Dimensionless temperature                           |
| $T$   | Temperature ( $K$ )                   | $u, v$               | Velocity components along with $x$ & $y$ directions |
| $T_w$ | Temperature at the plate ( $K$ )      | $U$                  | Dimensional free stream velocity                    |
| $n$   | Frequency                             | $C_\infty$           | Concentration away from the plate ( $mol m^{-3}$ )  |
| $Nu$  | Nusselt number                        | $C_w$                | Concentration at the plate ( $mol m^{-3}$ )         |
| $v_0$ | Suction velocity ( $m s^{-1}$ )       | $T_\infty$           | Temperature away from the plate ( $K$ )             |
| $U_0$ | Free stream velocity ( $m s^{-1}$ )   | <b>Greek symbols</b> |   |
| $q$   | Rate of heat flux                     | $\beta_T$            | Coefficient of thermal expansion                    |

|       |                                 |               |  |
|-------|---------------------------------|---------------|--|
| $C$   | Concentration ( $mol\ m^{-3}$ ) | $\alpha_c$    | Coefficient of concentration expansion   |
| $k$   | Permeability ( $m^3$ )          | $\beta$       | Phase of the heat flux                   |
| $B$   | Amplitude of suction velocity   | $\alpha$      | Phase of the skin friction               |
| $Pr$  | Prandtl number                  | $\varepsilon$ | perturbation parameter                   |
| $Gr$  | Grashof number                  | $\rho$        | Density ( $kg\ m^{-3}$ )                 |
| $G_s$ | Solutal Grashof number          | $\rho_0$      | Reference density                        |
| $E$   | Eckert number                   | $\tau$        | Skin friction                            |
| $Sc$  | Schmidt number                  | $k$           | Thermal diffusivity                      |
| $Sh$  | Sherwood number                 | $\bar{\nu}$   | Kinematic viscosity of the porous medium |
| $A$   | Amplitude of Suction velocity   | $\nu$         | Kinematic viscosity of the fluid         |

## 1. Introduction

A porous medium can be described as a solid or a series of solid materials (consists of pores or voids) with sufficient open space to allow fluid to move through or around the solids in or around them. The structure of the porous media may be at the microscopic level (i.e., the distribution of the pore size, the frequency of interconnectedness and inclination of the pores, the proportion of dead pores, etc.) or at the macroscopic stage (i.e., bulk parameters that have been averaged over scales much greater than the size of pores). The macroscopic approach is adequate for system development, where the greater importance is fluid flow, heat, and mass transfer, and the particle measurements are much shorter than the pore scale. In the fields of science and engineering, porous media play an important role (e.g., (i) In Soil Science: Soil transports water and nutrients to plants; (ii) Chemical Engineering: A filter or catalyst bed is used as a porous medium; (iii) Petroleum engineering: porous (reservoir rock) stores, crude stores, crude stores, etc.). Natural substances are referred to as permeable media, such as soils, rocks, bones, organic tissues, and artificial materials such as cement, foams, and stoneware. The physical characteristics of the fluid in the porous medium have countless applications with different surface geometries and boundary conditions such as nuclear waste management, the spread of pollutants, packed-bed reactors, petroleum reservoirs etc., which has attracted significant interest in recent decades.

In this respect, comprehensive reviews and literature are presented in recent books by Pop and Ingham [1], Nield and Bejan [2]. In saturated porous channels, convective heat transfer has attracted significant interest due to a broad range of applications in the last decades, like the underground spreading of chemical waste, thermal insulation engineering, water movement in geothermal reservoirs, improved recovery of oil reservoirs, grain storage, and nuclear waste repository, geothermal engineering. Jean *et al.* [3] elaborated Newtonian flows through a rigid body in the porous medium. Devakar *et al.* [4] examined Newtonian fluids through a porous and nonporous medium in a cylinder whereas, Veera Sankar *et al.* [5] discussed in between two vertical cylinders. Malleswari *et al.* [6] analyzed coupled effect of multi-slips and activation energy in a micropolar nanoliquid on a convectively heated elongated surface, and Satya Narayana *et al.* [7] examined the influence of chemical reaction on MHD couple stress nanoliquid flow over a bidirectional stretched sheet.

The progress of contemporary technology has necessitated the study of fluid streams, which encompass the interplay of various phenomena. Attention is focused here on multi-diffusive mixed convection. Transfer of heat and mass due to buoyancy effects are found in several certainly happening processes and multiple engineering applications. The study of these

progressions provides the imperative physical understanding and subsequently helps refine chemical technologies. In the last five decades, many authors (like Murthy *et al.* [8], Chamka [9], Mamou *et al.* [10], Kumari *et al.* [11], Patil *et al.* [12]) are showing considerable interest in the study of double-diffusive free, natural; mixed convection flows in a saturated porous medium from a vertical plate by considering different fields due to technological, geothermal, environmental issues and engineering applications. Owing to the vast number of applications in both industrial and technical areas, double diffusion arises in buoyancy forced flow due to the combination of temperature and concentration gradients. Numerous authors have investigated such research in a porous medium with varied geometries. Mallikarjuna *et al.* [13] tested the influence of non-uniform heating systems on a rotary device moving over a non-Darcy porous medium plate. Suresh Babu *et al.* [14] presented the findings of double-diffusive on mixed convective viscous fluid via a plate with changing fluid characteristics. Harish *et al.* [15] explored the effects of chemical and thermophoresis on MHD mixed convection flow over an inclined porous plate with variable suction.

In the literature, the words oscillatory and unsteady are commonly used to characterize flows in which velocity, pressure, or both are time-dependent. A periodic flow oscillating around a zero value is known as oscillatory flow. Oscillatory flow is constantly significant from a technological standpoint because of its numerous practical applications, such as the aerodynamics of a helicopter rotor or a fluttering airfoil, and a number of bio-engineering issues. Pathak *et al.* [16] employed fluctuating wall temperature to investigate the impact of radiation on unstable free convection flow restricted by an oscillating plate. Different problems involving free, forced, natural, and mixed convection have been studied due to many practical applications modeled and approximated in a porous medium for different geometries. Also, the study of mixed convection with free stream oscillations for couple stress, micropolar fluid, etc. are of first importance in many aerodynamic flow problems such as prediction of fluid flows over helicopter rotor blades, turbo machinery blades, aerofoil lift hysteresis at the stall, flutter phenomena involving in wings, etc. The study of such flows was discussed numerically by many researchers like Suresh Babu *et al.* [17], Mohammad [18], Rangasamy *et al.* [19], Begum *et al.* [20], Venkateswarlu *et al.* [21], Selimefendigil *et al.* [22], Swarnalathamma *et al.* [23], Makhalemele *et al.* [24], Pratibha *et al.* [25].

The impact of viscous dissipation is seen in powerful gravitational forces and processes on a large scale. The heat lost owing to viscous dissipation in the energy equation is insignificant and may be omitted. However, when the force of gravity is very strong, the viscous dissipative impacts cannot be disregarded. Due to significant deceleration and strong gravity fields, the viscous dissipation impact plays an essential role in mixed convection flows in different platforms. Suction has the effect of removing decelerated suspended particles from the inside of the boundary layer before they can have a chance to create segregation. Suction provides higher pressure rises on the outer portion of the aerofoil at high angles of incidence, resulting in considerably larger maximum lift values and minimizing drag. The injection is yet another way to prevent separation by adding energy to the flowing fluid stuck in the boundary layer by pumping fluid from the inner region of the boundary layer using a particular blower. With Newtonian fluids, Kamran *et al.* [26] investigated the effects of heat production and viscous dissipation on free convective flows through an impulsive vertical channel. Das *et al.* [27] illustrated the impact of radiation on unstable free convection flow through a vertical channel using Newtonian heating. Rajesh *et al.* [28] examined free convective flow over the surface, where the heat transfer rate from the surface is proportional to the current surface

temperature. Venkateswarlu *et al.* [29] studied melting and viscous dissipation effects on MHD flow over a moving surface with the constant heat source. Agarwal *et al.* [30] investigated the unstable mixed convective flow of an electrically conducting viscous fluid over a vertical porous plate with heat transfer characteristics is explored in two dimensions. Roy *et al.* [31] used the Oldroyd-B model to study the impact of double-diffusion and viscous dissipation on convective instability in a horizontal porous layer with a viscoelastic fluid. Using the Brinkman extended Darcy model, Dipak *et al.* [32] attempted to examine the influence of viscous dissipation on the onset convective instability in a horizontal porous layer of finite thickness confined within two permeable limits.

Applications of the moving field in the industry are among the most important phenomena for convective heat and mass transfer concepts. For instance, producing electric power is a process that involves extracting electrical energy directly from a flowing conducting field in the power sector. This study has been analyzed for different geometries and boundary layer approximations [33-38]. Ganesh *et al.* [33] discussed the study of unsteady MHD stokes flow between two parallel plates by considering one in uniform motion and the other plate at rest with uniform suction and angular velocity. Jiang *et al.* [34] studied double-diffusive convective flow under the influence of time-periodic sidewall temperature through a porous medium using numerical simulation and analytical prediction. Lazarus Rundora *et al.* [35] investigated thermal breakdown in an unsteady MHD flow of a reactive, electrically conducting Casson fluid inside a vertical plate filled with a porous material and the impact of temperature-dependent characteristics on the flow. Mahanta *et al.* [36] examined ramped wall temperature and concentration of an unsteady free MHD fluid past a vertical plate through a medium of porous nature under thermal radiation. Narsimlu *et al.* [37] investigated the effect of mass transfer on the unsteady MHD flow of a viscous fluid through an infinitely vertical plate with continuous suction and a heating element. Krishna *et al.* [38] investigated MHD flow involving heat and mass transfer characteristics under the influence of thermal radiation across an oscillating plate immersed in a Darcian porous material.

Much work has not been carried out in the literature for the unsteady model of mixed convection to study combined effects on fluctuation, free stream velocities, and viscous dissipation. Hence, the novelty of the present work is to analyze the combined effects of fluctuation, free stream velocities, and viscous dissipation on the unsteady mixed convective flow of an incompressible, laminar, Boussinesq flow embedded in a porous medium over a vertical plate analytically for various non-dimensional parameters which are involved in a physical model. In addition, a comparative study is adopted to validate our results for a particular case of the physical problem. The physical importance of boundary layer flow with suction and injection is critical in many engineering applications, particularly aerospace, chemical, and mechanical engineering.

## 2. Mathematical Formulation

Consider a 2D, mixed convective unsteady flow over a vertical porous plate bounded by a uniform homogeneous porous medium with a thin environment, time-dependent suction. In the Cartesian coordinate system, the  $x$ -axis is taken along the porous plate, which is exactly reverse to the gravitational force, and the  $y$ -axis is taken perpendicular to it. The geometry and its coordinate system of the problem are presented in Figure 1. Also, assume that the plate is kept at a constant temperature and moving with a free stream velocity  $U_0$ . The governing PDE's

are derived by assuming the fluid properties are invariant throughout the flow and taking Boussinesq approximation into account for the system [17].

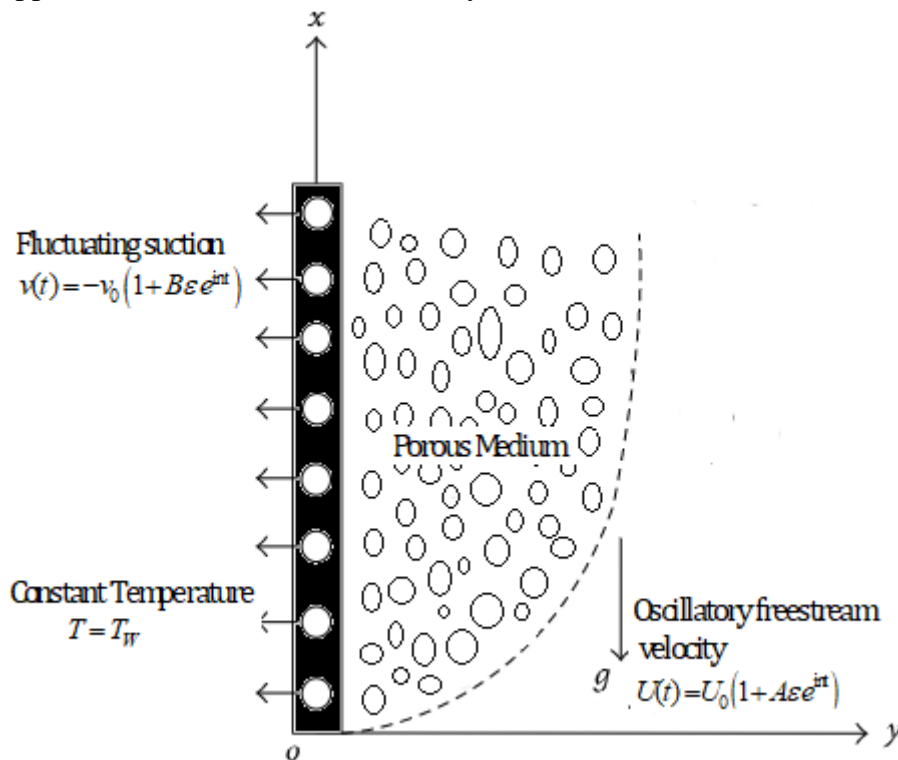


**Figure 1.** Sketch of the proposed coordinate system.

$$\frac{\partial v}{\partial y} = 0, \quad (1)$$

$$\frac{\partial u}{\partial t} + v \frac{\partial u}{\partial y} = \frac{dU}{dt} + v \frac{\partial^2 u}{\partial y^2} - \frac{\bar{v}}{k} (u - U) + \beta_T g (T - T_\infty) - \alpha_c g (C - C_\infty), \quad (2)$$

$$\frac{\partial T}{\partial t} + v \frac{\partial T}{\partial y} = \kappa \frac{\partial^2 T}{\partial y^2} + \frac{v}{C_p} \left( \frac{\partial u}{\partial y} \right)^2 + \frac{\bar{v}}{k C_p} (u - U_0)^2, \quad (3)$$

$$\frac{\partial C}{\partial t} + v \frac{\partial C}{\partial y} = D \frac{\partial^2 C}{\partial y^2}. \quad (4)$$

and its BC's are

$$y=0 : \quad u=0, \quad T=T_\infty, \quad C=C_\infty, \quad (5)$$

$$y \rightarrow \infty : \quad u \rightarrow U(t), \quad T \rightarrow T_\infty, \quad C \rightarrow C_\infty.$$

The irregular free-stream, as well as suction velocities [17], are defined according to the physical model as follows

$$U(t) = U_0 (1 + A\epsilon e^{int}) \text{ and } v(t) = -v_0 (1 + B\epsilon e^{int}), \quad (6)$$

where, "-" sign represents the suction is towards the porous plate. Now introducing the following dimensionless scheme

$$y^* = \frac{v_0 y}{\nu}, \quad u^* = \frac{u}{U_0}, \quad v^* = \frac{v}{v_0}, \quad n^* = \frac{\nu n}{v_0^2}, \quad y^* = \frac{v_0 y}{\nu}, \quad Gr = \frac{\beta_T v_0 g (T_w - T_\infty)}{U_0 \nu_0^2}, \quad Gr = \frac{\alpha_c v_0 g (C_w - C_\infty)}{U_0 \nu_0^2}, \quad (7)$$

$$\theta = \frac{(T - T_\infty)}{(T_w - T_\infty)}, \quad t^* = \frac{v_0^2 t}{\nu}, \quad Pr = \frac{\nu}{\kappa}, \quad Sc = \frac{\nu}{\sigma}, \quad k = \frac{\nu^2 k^*}{v_0^2}, \quad \phi = \frac{(C - C_\infty)}{(C_w - C_\infty)}, \quad E = \frac{U_0^2}{C_p (T_w - T_\infty)}.$$

The flow equations (1) - (4) and the corresponding BC's (5) in the dimensionless form are,

$$\frac{\partial u}{\partial t} - v_0 (1 + B\epsilon e^{int}) \frac{\partial u}{\partial y} = \frac{dU}{dt} + \frac{\partial^2 u}{\partial y^2} + \frac{\lambda}{k} (U - u) + Gr \theta - Gs \theta, \quad (8)$$

$$\frac{\partial \theta}{\partial t} - v_0 (1 + B \varepsilon e^{\text{int}}) \frac{\partial \theta}{\partial y} = \frac{1}{\text{Pr}} \frac{\partial^2 \theta}{\partial y^2} + E \left( \left( \frac{\partial \theta}{\partial y} \right)^2 + \frac{\lambda}{k} (u - U_0)^2 \right), \quad (9)$$

$$\frac{\partial \phi}{\partial t} - v_0 (1 + B \varepsilon e^{\text{int}}) \frac{\partial \phi}{\partial y} = \frac{1}{\text{Sc}} \frac{\partial^2 \phi}{\partial y^2}, \quad (10)$$

$$\begin{aligned} y=0 : \quad & u=0; \quad \theta=1; \quad \phi=1, \\ y \rightarrow \infty : \quad & u \rightarrow (1 + \varepsilon A e^{\text{int}}); \quad \theta \rightarrow 0; \quad \phi \rightarrow 0. \end{aligned} \quad (11)$$

### 3. Method of Solution

A regular perturbation technique is used to solve the equations (8) - (10) along with the BC's (11)

$$u(y, t) = u_0(y) + \varepsilon u_1(y) e^{\text{int}} + O(\varepsilon^2), \quad (12)$$

$$\theta(y, t) = \theta_0(y) + \varepsilon \theta_1(y) e^{\text{int}} + O(\varepsilon^2), \quad (13)$$

$$\phi(y, t) = \phi_0(y) + \varepsilon \phi_1(y) e^{\text{int}} + O(\varepsilon^2). \quad (14)$$

Comparing the coefficient of  $\varepsilon^0$  terms, after substituting equations (12), (13), and (14) in (8) to (10), we get

$$u_0'' + u_0' - \frac{\lambda}{k} u_0 = Gs \phi_0 - Gr \theta_0 - \frac{\lambda}{k}, \quad (15)$$

$$\theta_0'' + \text{Pr} \theta_0' = -E \text{Pr} \left\{ (u_0')^2 + \frac{\lambda}{k} u_0^2 \right\}, \quad (16)$$

$$\phi_0'' + \text{Sc} \phi_0' = 0. \quad (17)$$

The corresponding boundary conditions are

$$y=0 : \quad u_0=0; \quad \theta_0=1; \quad \phi_0=1, \quad (18)$$

$$y \rightarrow \infty : \quad u_0 \rightarrow 1; \quad \theta_0=0; \quad \phi_0=0.$$

Comparing the coefficient of  $\varepsilon^1$  terms, we get

$$u_1'' + u_1' - \left( in + \frac{\lambda}{k} \right) u_1 = Gs \phi_1 - Gr \theta_1 - B u_0' - A \left( in + \frac{\lambda}{k} \right), \quad (19)$$

$$\theta_1'' + \text{Pr} \theta_1' - in \text{Pr} \theta_1 = -2E \text{Pr} \left( u_0' u_1' + \frac{\lambda}{k} u_0 u_1 \right) - B \text{Pr} \theta_0', \quad (20)$$

$$\phi_1'' + \text{Sc} \phi_1' - in \text{Sc} \phi_1 = -B \text{Sc} \phi_0'. \quad (21)$$

The corresponding boundary conditions are

$$y=0 : \quad u_1=0; \quad \theta_1=1; \quad \phi_1=1, \quad (22)$$

$$y \rightarrow \infty : \quad u_1 \rightarrow A; \quad \theta_1=0; \quad \phi_1=0.$$

Equations (15), (16), (17), (19), (20), and (21) are coupled, hence by solving considering  $E$  is very small.

$$u_0(y) = u_{00}(y) + E u_{01}(y) + O(E^2), \quad (23)$$

$$u_1(y) = u_{11}(y) + E u_{12}(y) + O(E^2), \quad (24)$$

$$\theta_0(y) = \theta_{00}(y) + E \theta_{01}(y) + O(E^2), \quad (25)$$

$$\theta_1(y) = \theta_{11}(y) + E \theta_{12}(y) + O(E^2), \quad (26)$$

$$\phi_0(y) = \phi_{00}(y) + E \phi_{01}(y) + O(E^2), \quad (27)$$

$$\phi_1(y) = \phi_{11}(y) + E \phi_{12}(y) + O(E^2). \quad (28)$$

Comparing the coefficient of  $E^0$  terms after substituting equations (23), (25) and (27) in (15), (16) and (17), we get



$$u''_{00} + u'_{00} - \frac{\lambda}{k} u_{00} = Gs \phi_{00} - Gr \theta_{00} - \frac{\lambda}{k}, \quad (29)$$

$$\theta''_{00} + Pr \theta'_{00} = 0, \quad (30)$$

$$\phi''_{00} + \beta \phi'_{00} = 0, \quad (31)$$

and the subsequent BC's are

$$y=0 : u_{00}=0; \quad \theta_{00}=1; \quad \phi_{00}=1, \quad (32)$$

$$y \rightarrow \infty : u_{00} \rightarrow 1; \quad \theta_{00} \rightarrow 0; \quad \phi_{00} \rightarrow 0.$$

Comparing the coefficient of  $E^1$  terms, we get

$$u''_{01} + u'_{01} - \frac{\lambda}{k} u_{01} = Gs \phi_{01} - Gr \theta_{01}, \quad (33)$$

$$\theta''_{01} + Pr \theta'_{01} = -Pr (u'_{00})^2 - \frac{\lambda}{k} Pr u_{00}^2, \quad (34)$$

$$\phi''_{01} + \beta \phi'_{01} = 0, \quad (35)$$

and the subsequent BC's are

$$y=0 : u_{01}=0; \quad \theta_{01}=1; \quad \phi_{01}=1, \quad (36)$$

$$y \rightarrow \infty : u_{01} \rightarrow 0; \quad \theta_{01} \rightarrow 0; \quad \phi_{01} \rightarrow 0.$$

Similarly, Comparing the coefficient of  $E^0$  terms after substituting equations (24), (26) and (28) in (19),(20) and (21), we get

$$u''_{11} + u'_{11} - (in + \frac{\lambda}{k}) u_{11} = Gs \phi_{11} - Gr \theta_{11} - A \left( in + \frac{\lambda}{k} \right) - B u'_{00}, \quad (37)$$

$$\theta''_{11} + Pr \theta'_{11} - in Pr \theta_{11} = -B Pr \theta'_{00}, \quad (38)$$

$$\phi''_{11} + \beta \phi'_{11} - in Sc \phi_{11} = -B Sc \phi'_{00}, \quad (39)$$

and the subsequent BC's are

$$y=0 : u_{11}=0, \quad \theta_{11}=0, \quad \phi_{11}=0, \quad (40)$$

$$y \rightarrow \infty : u_{11} \rightarrow A, \quad \theta_{11} \rightarrow 0, \quad \phi_{11} \rightarrow 0.$$

Comparing the coefficient of  $E^1$  terms, we get

$$u''_{12} + u'_{12} - (in + \frac{\lambda}{k}) u_{12} = Gs \phi_{12} - Gr \theta_{12} - B u'_{01}, \quad (41)$$

$$\theta''_{12} + Pr \theta'_{12} - in Pr \theta_{12} = -Pr B \theta'_{01} - 2 Pr \left( u'_{00} u'_{11} + \frac{\lambda}{k} u_{00} u_{11} \right), \quad (42)$$

$$\phi''_{12} + Sc \phi'_{12} - in c Sc \phi_{12} = -B Sc \phi'_{01}, \quad (43)$$

and the subsequent BC's are

$$y=0 : u_{12}=0, \quad \theta_{12}=0, \quad \phi_{12}=0, \quad (44)$$

$$y \rightarrow \infty : u_{12} \rightarrow 0, \quad \theta_{12} \rightarrow 0, \quad \phi_{12} \rightarrow 0.$$

The final equations are as follows after solving the above equations, we get

$$\begin{aligned} u(y,t) = & [(1 + A_1 e^{-pr y} + A_2 e^{-Sc y} + A_3 e^{-m_2 y}) + E(A_4 e^{-pr y} + A_5 e^{-2pr y} + A_6 e^{-2Sc y} + A_7 e^{-2m_2 y} + A_8 e^{-Sc y} \\ & + A_9 e^{-(pr+Sc)y} + A_{10} e^{-(Sc+m_2)y} + A_{11} e^{-(pr+m_2)y} + A_{12} e^{-m_2 y})] + \epsilon \{ [(A_{13} e^{-pr y} + A_{14} e^{-Sc y} + A_{15} \\ & + A_{16} e^{-m_4 y} + A_{17} e^{-m_6 y} + A_{18} e^{-m_8 y}) + [A_{19} + A_{20} e^{-m_2 y} + A_{21} e^{-m_4 y} + A_{22} e^{-m_6 y} + A_{23} e^{-m_8 y} + A_{24} e^{-2m_2 y} \\ & + A_{25} e^{-(m_2+m_4)y} + A_{26} e^{-(m_2+m_6)y} + A_{27} e^{-(m_2+m_8)y} + A_{28} e^{-(m_2+pr)y} + A_{29} e^{-(pr+m_4)y} + A_{30} e^{-(pr+m_6)y} \\ & + A_{31} e^{-(pr+m_8)y} + A_{32} e^{-pr y} + A_{33} e^{-2pr y} + A_{34} e^{-Sc y} + A_{35} e^{-(pr+Sc)y} + A_{36} e^{-(m_2+Sc)y} + A_{37} e^{-(m_4+Sc)y} \\ & + A_{38} e^{-(m_6+Sc)y} + A_{39} e^{-(m_8+Sc)y} + A_{40} e^{-2Sc y}] \} e^{\text{int}} + O(\epsilon^2) \end{aligned} \quad (45)$$

$$\begin{aligned} \theta(y,t) = & [e^{-pr y} + E(B_1 e^{-2pr y} + B_2 e^{-2Sc y} + B_3 e^{-2m_2 y} + B_4 e^{-Sc y} + B_5 e^{-m_2 y} + B_6 e^{-(pr+Sc) y} \\ & + B_7 e^{-(m_2+Sc) y} + B_8 e^{-(pr+m_2) y} + B_9 e^{-pr y})] + \in \{ [B_{10} (e^{-pr y} - e^{-m_4 y}) + E(B_{11} + B_{12} e^{-m_2 y} \\ & + B_{13} e^{-m_6 y} + B_{14} e^{-m_8 y} + B_{15} e^{-2m_2 y} + B_{16} e^{-(m_2+m_4) y} + B_{17} e^{-(m_2+m_6) y} + B_{18} e^{-(m_2+m_8) y} \\ & + B_{19} e^{-(m_2+pr) y} + B_{20} e^{-(m_4+pr) y} + B_{21} e^{-(pr+m_6) y} + B_{22} e^{-(pr+m_8) y} + B_{23} e^{-pr y} + B_{24} e^{-2pr y} \\ & + B_{25} e^{-Sc y} + B_{26} e^{-(Sc+pr) y} + B_{27} e^{-(m_2+Sc) y} + B_{28} e^{-(m_4+Sc) y} + B_{29} e^{-(m_6+Sc) y} + B_{30} e^{-(m_8+Sc) y} \\ & + B_{31} e^{-2Sc y} + B_{32} e^{-m_4 y})] \} e^{\text{int}} + O(\varepsilon^2). \end{aligned} \quad (46)$$

$$\phi(y,t) = e^{-Sc y} + E(C_1 e^{-Sc y} - C_1 e^{-m_6 y}) e^{\text{int}} + O(\varepsilon^2). \quad (47)$$

$$\text{where } m_{1,2} = \frac{-1 \pm \sqrt{1 + 4 \frac{\lambda}{k}}}{2} = m_{7,8}; \quad m_{3,4} = \frac{-\text{Pr} \pm \sqrt{\text{Pr}^2 + 4 \text{Pr} in}}{2};$$

$$m_{5,6} = \frac{-be \pm \sqrt{be^2 + 4in \text{Pr}}}{2}; \quad m_{9,10} = \frac{-1 \pm \sqrt{1 + 4 \left( \frac{\lambda}{k} + in \right)}}{2}.$$

Here,  $A_i$  ( $i=1$  to  $40$ ),  $B_j$  ( $j=1$  to  $32$ ) and  $C_l$  are all constants involved in the problem. The expressions are mentioned in the appendix section and used for computing  $u$ ,  $\theta$  and  $\phi$ . The skin friction and heat flux can be evaluated in the non-dimensional form as follows near the plate

$$\begin{aligned} \tau = \left( \frac{du}{dy} \right)_{y=0} &= \left( \frac{du_0}{dy} + \varepsilon e^{\text{int}} \frac{du_1}{dy} \right)_{y=0} = \left( \frac{du}{dy} \right)_{y=0} + \varepsilon |L| \cos(nt + \alpha), \\ Nu = \left( \frac{d\theta}{dy} \right)_{y=0} &= \left( \frac{d\theta_0}{dy} \right)_{y=0} + \varepsilon e^{\text{int}} \left( \frac{d\theta_1}{dy} \right)_{y=0} = \left( \frac{d\theta_0}{dy} \right)_{y=0} + \varepsilon |Q| \cos(nt + \beta), \end{aligned}$$

where,  $|L|$  = amplitude of the skin friction,  $|Q|$  = amplitude of heat flux,

$\tan \alpha = \left( \frac{L_i}{L_r} \right)$  is the phase of the skin friction, and  $\tan \beta = \left( \frac{Q_i}{Q_r} \right)$  is the phase of the heat flux.

#### 4. Results and Discussion

An analytical solution has been carried out for the fluid characteristics under the influence of thermal and solutal Grashof numbers ( $Gr$  &  $G_s$ ), Prandtl number ( $Pr$ ), amplitude of the fluctuating suction velocity ( $B$ ), the amplitude of fluctuating free stream velocity ( $A$ ), permeability parameter ( $K$ ), and Eckert number ( $E$ ). The physical interpretation of the fluid is illustrated with the help of plots from Figs.2 to 14 of the physical model. Also, a comparative study has been done for  $G_s$  and  $Sc$  effects on skin friction, Nusselt and Sherwood numbers with Chamkha[9] in the non-appearance of magnetic field and heat absorption of the physical system and found that an excellent agreement from Tables 1 and 2. From Table 1, we observed that as the solutal Grashof number  $G_s$  enhances, the skin friction coefficient increases, and the heat and mass transfer coefficients remain unaltered. Also, it is seen from Table 2, as Schmidt number enhances, there is a reduction in the skin friction and mass transfer coefficient, while the heat transfer coefficient remains the same.



#### 4.1. Effect of thermal Grashof Number ( $Gr$ ).

The behaviors of velocity, temperature, and concentration are obtained for both positive and negative values of  $Gr$  in Figures 2 and 3. Here,  $Gr > 0$  and  $Gr < 0$  represent the plate's cooling and heating. Figure 2 illustrates that the increase in  $Gr$  (both negative and positive values) increases the velocity for a particular value of  $Pr$  which is less than one due to enhancement of the buoyancy force. The graphs show that the velocity starts from the least value and enhances until the maximum value reaches the plate and decreases until the boundary layer's end. This is due to the channeling effect of the boundary layer of the plate and also due to suction at the plate. The positive values of  $Gr$ , the velocity enhances quickly near the plate and then decreases to the free stream velocity, and for negatives, there is a retardation in the velocity. The temperature distribution is depicted in Figure 3 for different positive and negative values of  $Gr$  and seen that the temperature increases as  $Gr$  it increases. The computational results revealed that there is not much significant variation in the case of concentration.

#### 4.2. Effect of Solutal Grashof Number ( $G_s$ ).

The velocity and temperature profiles for various values of solutal Grashof number  $G_s$  are presented in Figures 4 and 5. It can be seen that with an enhancement in the variation of  $G_s$ , which is due to reduction in the viscosity or exchange of concentration between the plate and far away from the boundary, it increases the variation of velocity as depicted in Figure 4. The percentage of variation velocity is more in the case of  $Gr$  as compared with  $G_s$ . An opposite behavior in reduction of temperature is seen in Figure 5 with the enhancement due to  $G_s$ . This is due to higher concentration  $C_w$  at the plate from the far away boundary concentration  $C_\infty$ , hence the fluid experiences higher density at the plate.

#### 4.3. Effect of Prandtl Number ( $Pr$ ).

The velocity variation from air to mercury is shown in Figure 6, and it is observed that the velocity decays due to enhancement in the variation of Prandtl number  $Pr$ . This indicates in experiment observation that the higher viscosity of the fluid flow will restrict at the moment because of the thickness of the fluid increases. The variation in velocity is large for  $Pr = 0.71$  to 3 and is very less  $Pr > 3$  due to viscous dissipation. Figure 7 shows that the temperature variation for distinct values of  $Pr$  and is seen that the temperature decays gradually with an increase in  $Pr$ . This indicates that higher viscosity of the fluid will reduce its thermal conductivity and lower the fluid temperature.

#### 4.4. Effect of Schmidt Number ( $Sc$ ).

The graphical explanation of the flow fields for the several values of  $Sc$  is highlighted in Figures 8 and 9. As the Schmidt number  $Sc$  increases, the fluid velocity and concentration decrease due to solutal diffusivity of the fluid, which leads to a higher density of the fluid particle. This reduces the momentum and velocity of the fluid. It has been observed that the percentage of reduction is more in the case of concentration profile than that of velocity due to solutal diffusivity, and much variation is not seen in the case of temperature.

#### 4.5. Effect of Amplitude of Suction Velocity Parameter ( $B$ ).

Figures 10-12 elaborate the variations of fluid characteristics for different values of the suction velocity parameter  $B$ , respectively. Figures 10 & 11 indicate that, as increasing the amplitude of the suction velocity  $v(t)$  due to the channeling effect of the permeable vertical plate, there is an enhancement in the velocity and temperature profiles. An opposite behavior is depicted in Figure 12 for the concentration profile due to the higher momentum of the fluid particle at the permeable vertical plate.

#### 4.6. Effect of Eckert Number ( $E$ ).

The effect of viscous dissipation is seen through variation in the non-dimensional parameter  $E$  in Figures 13 and 14.

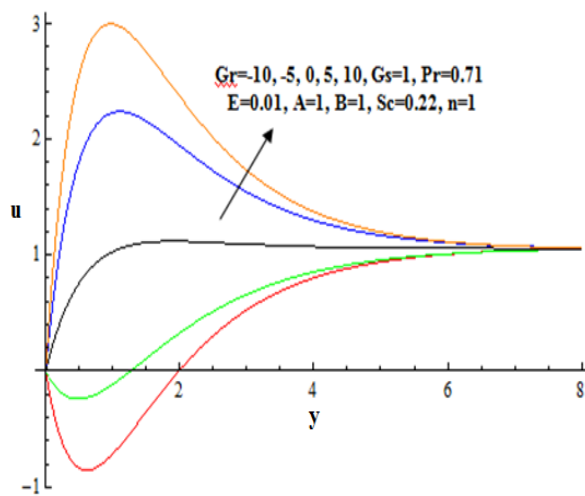


**Figure 2.** Impact of thermal Grashof number on velocity.

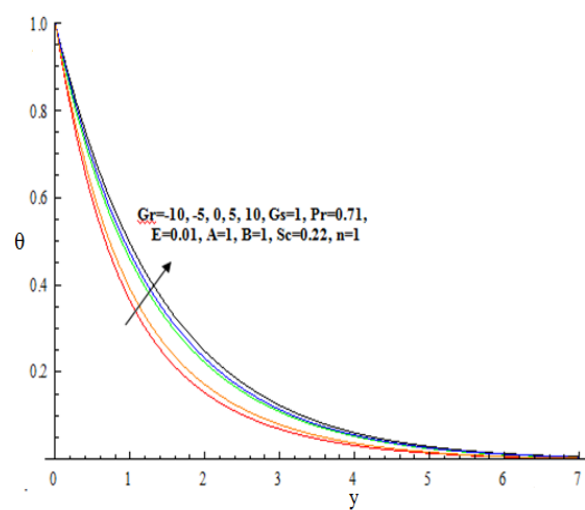


**Figure 3.** Impact of thermal Grashof number on temperature.

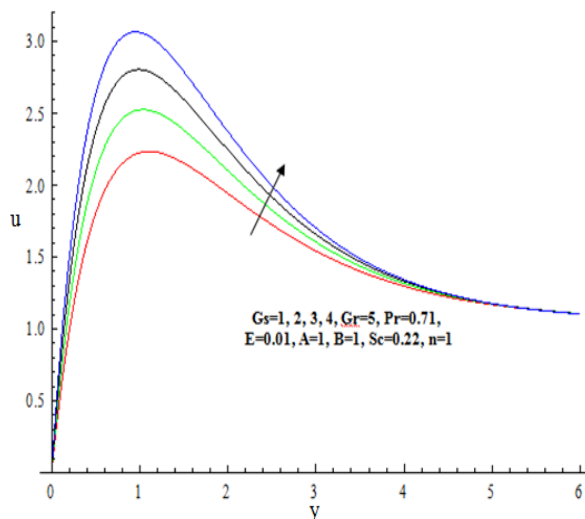


**Figure 4.** Impact of solutal Grashof number on velocity.

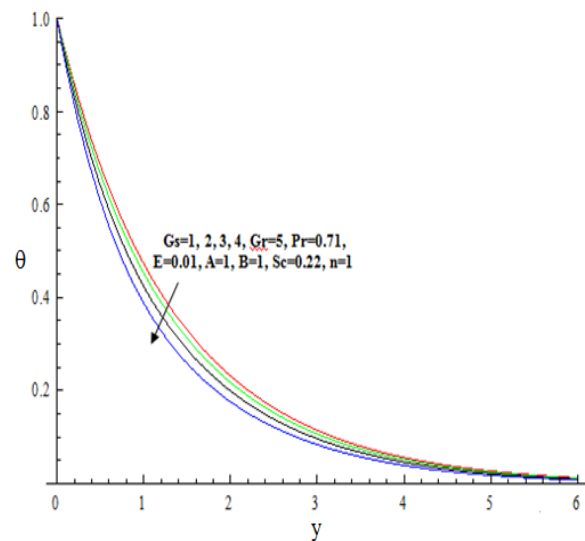


**Figure 5.** Impact of solutal Grashof number on temperature.

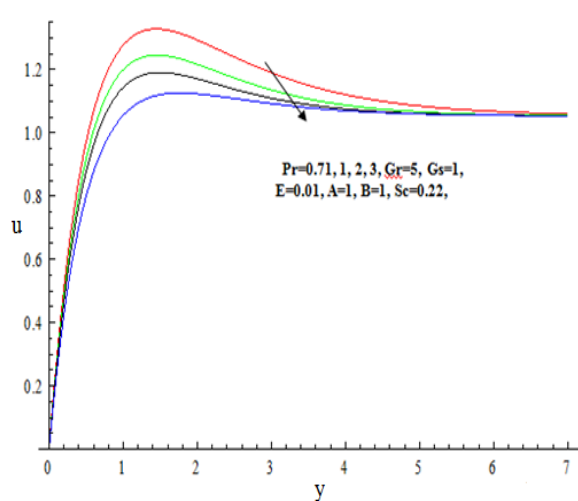


**Figure 6.** Impact of Prandtl number on velocity.

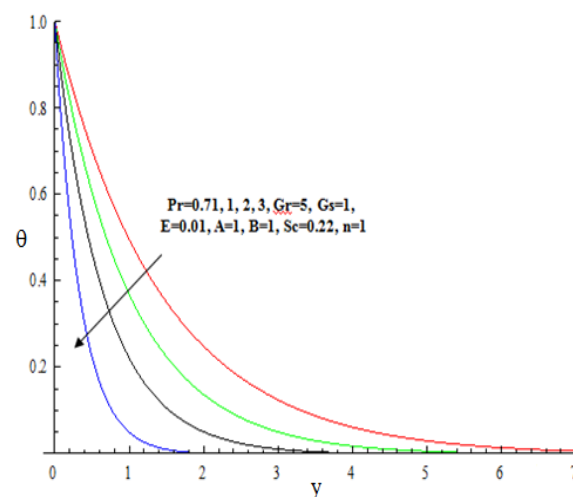


**Figure 7.** Impact of Prandtl number on temperature.

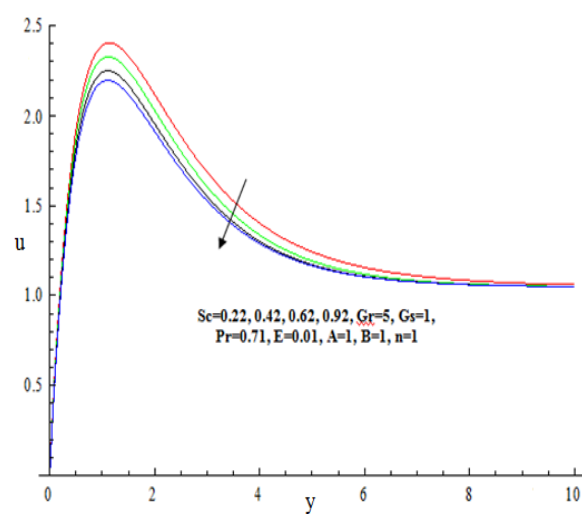


**Figure 8.** Impact of Schmidt number on velocity.

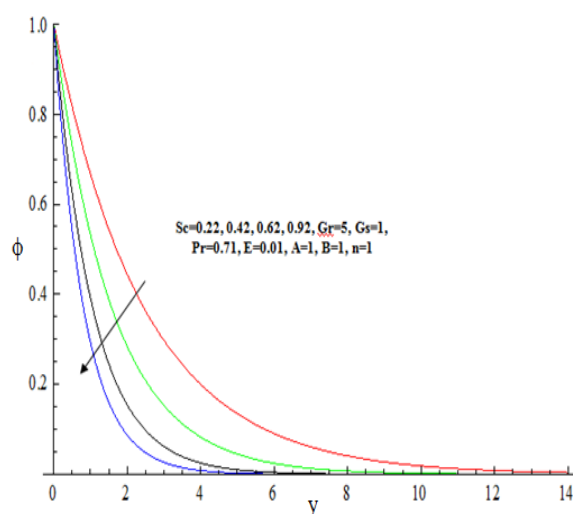


**Figure 9.** Impact of Schmidt number on concentration.

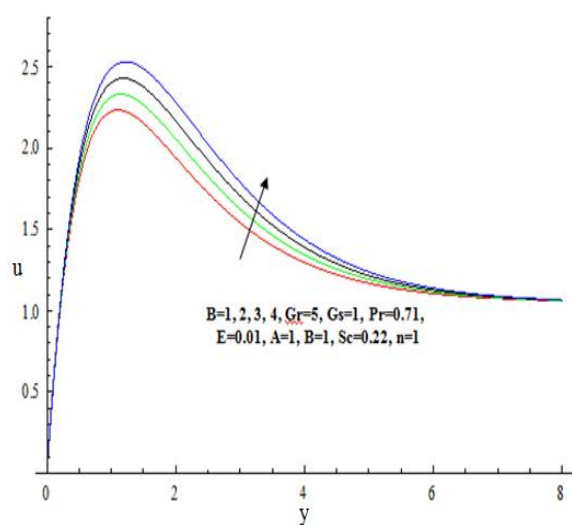


**Figure 10.** Impact of suction velocity parameter on velocity.

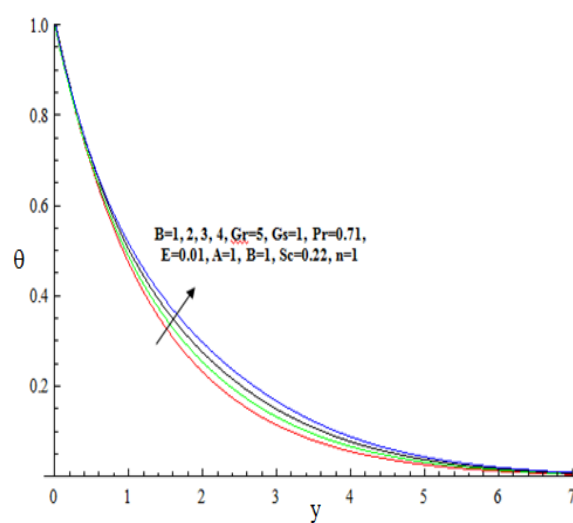


**Figure 11.** Impact of suction velocity parameter on temperature.

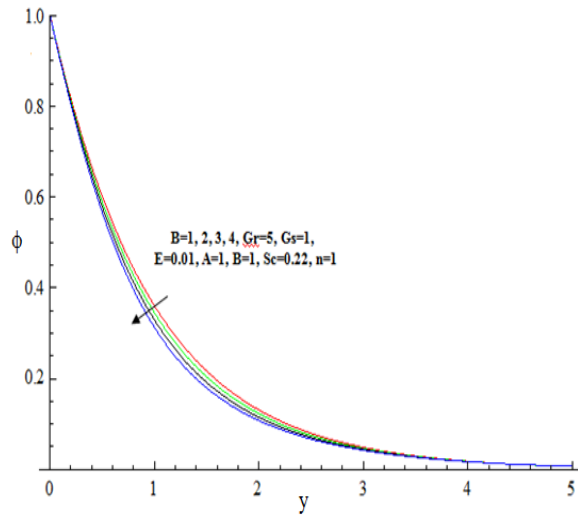


**Figure 12.** Impact of suction velocity parameter on concentration.

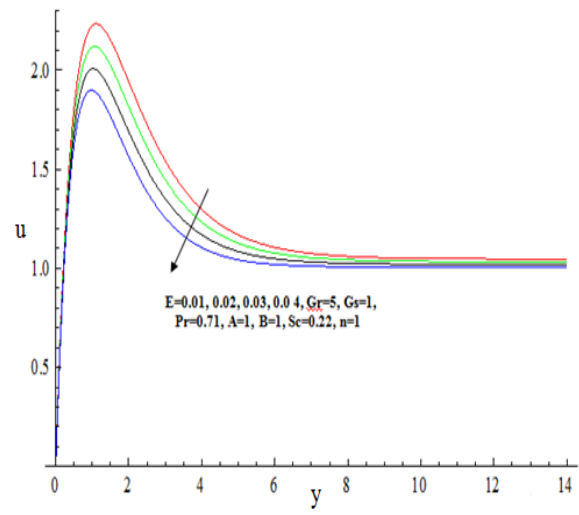


**Figure 13.** Impact of Eckert Number on velocity.

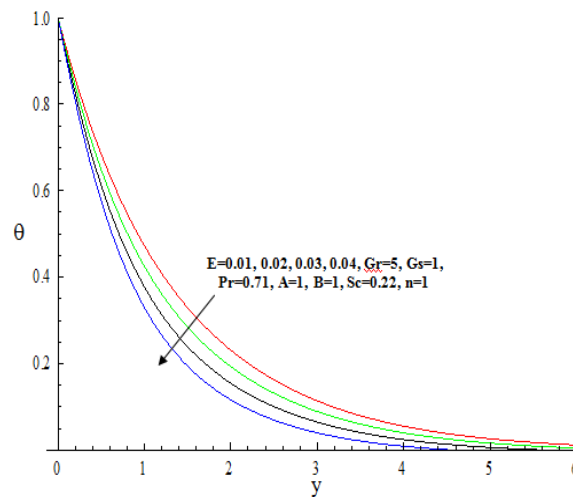


**Figure 14.** Impact of Eckert Number on temperature.

The small variation of  $E$  will lead to a decrease in velocity and as well as temperature. From Figure 13, it is observed that as increasing viscous dissipation, the velocity of the fluid decreases moderately near the vertical permeable plate and becomes constant away from the plate. This is true because increasing  $E$  will cause the temperature due to the temperature difference between the plate and far away from the fluid. The temperature will transfer from the plate to the far away fluid since the plate is maintained higher temperature. Hence the velocity increases due to thermal buoyancy forces.

**Table 1.** Comparison of the results obtained with that of Chamkha [9].

| $G_s$ | Chamkha[ 9 ] |         |         | Present results ( $10^{-6}$ ) |           |           |
|-------|--------------|---------|---------|-------------------------------|-----------|-----------|
|       | $\tau$       | $Nu$    | $Sh$    | $\tau$                        | $Nu$      | $Sh$      |
| 0     | 2.7200       | -1.7167 | -0.8098 | 2.720010                      | -1.716701 | -0.809812 |
| 1     | 3.2772       | -1.7167 | -0.8098 | 3.277162                      | -1.716701 | -0.809812 |
| 2     | 3.8343       | -1.7167 | -0.8098 | 3.834251                      | -1.716701 | -0.809812 |
| 3     | 4.3915       | -1.7167 | -0.8098 | 4.391501                      | -1.716701 | -0.809812 |
| 4     | 4.9487       | -1.7167 | -0.8098 | 4.948683                      | -1.716701 | -0.809812 |

**Table 2.** Comparison of the results obtained with that of Chamkha [9].

| <i>Sc</i> | Chamkha[ 9 ] |           |           | Present results (10 <sup>-6</sup> ) |           |           |
|-----------|--------------|-----------|-----------|-------------------------------------|-----------|-----------|
|           | $\tau$       | <i>Nu</i> | <i>Sh</i> | $\tau$                              | <i>Nu</i> | <i>Sh</i> |
| 0.16      | 3.4328       | -1.7167   | -0.2231   | 3.432803                            | -1.716701 | -0.223052 |
| 0.6       | 3.2772       | -1.7167   | -0.8098   | 3.277197                            | -1.716701 | -0.809802 |
| 1         | 3.1847       | -1.7167   | -1.3425   | 3.184700                            | -1.716701 | -1.342687 |
| 2         | 4.0481       | -1.7167   | -2.6741   | 4.048154                            | -1.716701 | -2.674113 |

## 5. Conclusions

The conclusions from this study can be listed as follows: (i) As *Gr* enhances, the velocity temperature fields increases and the effect is significantly less on concentration distribution; (ii) The velocity increases and temperature decreases as *Gs* enhances; (iii) As Prandtl number increases, the velocity, and temperature decreases and there is no effect on the concentration profile; (iv) As Schmidt number increases, the velocity and concentration profiles decreases; (v) As fluctuating free stream velocity parameter increases, the velocity, temperature increases, and concentration decreases; (vi) As Eckert number increases, the velocity and temperature profiles decreases.

## Appendix

$$\begin{aligned}
 A_1 &= \frac{-Gr}{Pr^2 - Pr - \sigma}; A_2 = \frac{-Gs}{Sc^2 - Sc - \sigma}; A_3 = -(1 + A_1 + A_2); A_4 = \frac{-Gr g_{33}}{Pr^2 - Pr - \sigma}; A_5 = \frac{-Gr g_{25}}{4Pr^2 - 2Pr - \sigma}; \\
 A_6 &= \frac{-Gr g_{26}}{4Sc^2 - 2Sc - \sigma}; A_7 = \frac{-Gr g_{27}}{4m_2^2 - 2m_2 - \sigma}; A_8 = \frac{-Gr g_{28}}{Sc^2 - Sc - \sigma}; A_9 = \frac{-Gr g_{30}}{(Sc + Pr)^2 - (Sc + Pr) - \sigma}; \\
 A_{10} &= \frac{-Gr g_{31}}{(Sc + m_2)^2 - (Sc + m_2) - \sigma}; A_{12} = \frac{-Gr g_{29}}{m_2^2 - m_2 - \sigma}; A_{11} = \frac{-Gr g_{32}}{(Pr + m_2)^2 - (Pr + m_2) - \sigma}; A_{13} = \frac{g_6}{Pr^2 - Pr - \omega}; \\
 A_{14} &= \frac{g_7}{Sc^2 - Sc - \omega}; A_{15} = \frac{-g_8}{(in + \sigma)}; A_{16} = \frac{Gr g_4}{m_4^2 - m_4 - \omega}; A_{17} = \frac{Gr g_5}{m_6^2 - m_6 - \omega}; A_{18} = -(g_9 + \dots + g_{13}); \\
 A_{19} &= \frac{-g_{90}}{\omega}; A_{20} = \frac{g_{91}}{m_2^2 - m_2 - \omega}; A_{21} = \frac{g_{92}}{m_4^2 - m_4 - \omega}; A_{22} = \frac{g_{93}}{m_6^2 - m_6 - \omega}; A_{23} = \frac{g_{94}}{m_8^2 - m_8 - \omega}; \\
 A_{24} &= \frac{g_{95}}{4m_2^2 - 2m_2 - \omega}; A_{26} = \frac{g_{97}}{(m_2 + m_6)^2 - (m_2 + m_6) - \omega}; A_{27} = \frac{g_{98}}{(m_2 + m_8)^2 - (m_2 + m_8) - \omega}; \\
 A_{28} &= \frac{g_{99}}{(m_2 + Pr)^2 - (m_2 + Pr) - \omega}; A_{29} = \frac{f_1}{(m_4 + Pr)^2 - (m_4 + Pr) - \omega}; A_{30} = \frac{f_2}{(m_6 + Pr)^2 - (m_6 + Pr) - \omega}; \\
 A_{31} &= \frac{f_3}{(m_8 + Pr)^2 - (m_8 + Pr) - \omega}; A_{32} = \frac{f_4}{Pr^2 - Pr - \omega}; A_{33} = \frac{f_5}{4Pr^2 - 2Pr - \omega}; A_{34} = \frac{f_6}{Sc^2 - Sc - \omega}; \\
 A_{35} &= \frac{f_7}{(Pr + Sc)^2 - (Pr + Sc) - \omega}; A_{36} = \frac{f_8}{(m_2 + Sc)^2 - (m_2 + Sc) - \omega}; A_{37} = \frac{f_9}{(m_4 + Sc)^2 - (m_4 + Sc) - \omega}; \\
 A_{38} &= \frac{f_{10}}{(m_6 + Sc)^2 - (m_6 + Sc) - \omega}; A_{39} = \frac{f_{11}}{(m_8 + Sc)^2 - (m_8 + Sc) - \omega}; A_{40} = \frac{f_{12}}{4Sc^2 - 2Sc - \omega}; B_1 = \frac{g_{16}}{2Pr^2}; \\
 B_2 &= \frac{g_{17}}{4Ps^2 - 2Pr Sc}; B_3 = \frac{g_{18}}{4m_2^2 - 2Pr m_2}; B_4 = \frac{g_{20}}{Sc^2 - Pr Sc}; B_5 = \frac{g_{21}}{m_2^2 - Pr m_2}; \\
 B_6 &= \frac{g_{22}}{(Pr + Sc)^2 - Pr(Pr + Sc)}; B_{10} = \frac{-BPr}{in}; B_7 = \frac{g_{23}}{(Sc + m_2)^2 - Pr(Sc + m_2)}; B_8 = \frac{g_{24}}{(Pr + m_2)^2 - Pr(Pr + m_2)};
 \end{aligned}$$

$$\begin{aligned}
 B_9 &= -(g_{25} + \dots + g_{32}); B_{12} = \frac{g_{45}}{m_2^2 - \text{Pr } m_2 - i n \text{Pr}}; B_{13} = \frac{g_{47}}{m_6^2 - \text{Pr } m_6 - i n \text{Pr}}; B_{15} = \frac{g_{49}}{4m_2^2 - 2\text{Pr } m_2 - i n \text{Pr}}; \\
 B_{16} &= \frac{g_{50}}{(m_2 + m_4)^2 - \text{Pr}(m_2 + m_4) - i n \text{Pr}}; B_{17} = \frac{g_{51}}{(m_2 + m_6)^2 - \text{Pr}(m_2 + m_6) - i n \text{Pr}}; \\
 B_{18} &= \frac{g_{52}}{(m_2 + m_8)^2 - \text{Pr}(m_2 + m_8) - i n \text{Pr}}; B_{19} = \frac{g_{53}}{(m_2 + \text{Pr})^2 - \text{Pr}(m_2 + \text{Pr}) - i n \text{Pr}}; \\
 B_{20} &= \frac{g_{54}}{(m_4 + \text{Pr})^2 - \text{Pr}(m_4 + \text{Pr}) - i n \text{Pr}}; B_{21} = \frac{g_{55}}{(m_6 + \text{Pr})^2 - \text{Pr}(m_6 + \text{Pr}) - i n \text{Pr}}; B_{23} = \frac{g_{57}}{-i n \text{Pr}}; \\
 B_{22} &= \frac{g_{56}}{(m_8 + \text{Pr})^2 - \text{Pr}(m_8 + \text{Pr}) - i n \text{Pr}}; B_{24} = \frac{g_{58}}{2\text{Pr}^2 - i n \text{Pr}}; B_{25} = \frac{g_{59}}{Sc^2 - \text{Pr } Sc - i n \text{Pr}}; \\
 B_{26} &= \frac{g_{60}}{(Sc + \text{Pr})^2 - \text{Pr}(Sc + \text{Pr}) - i n \text{Pr}}; B_{27} = \frac{g_{61}}{(Sc + m_2)^2 - \text{Pr}(Sc + m_2) - i n \text{Pr}}; \\
 B_{28} &= \frac{g_{62}}{(Sc + m_4)^2 - \text{Pr}(Sc + m_4) - i n \text{Pr}}; B_{29} = \frac{g_{63}}{(Sc + m_6)^2 - \text{Pr}(Sc + m_6) - i n \text{Pr}}; \\
 B_{30} &= \frac{g_{64}}{(Sc + m_8)^2 - \text{Pr}(Sc + m_8) - i n \text{Pr}}; B_{31} = \frac{g_{65}}{4Sc^2 - 2\text{Pr } Sc - i n \text{Pr}}; B_{32} = -(g_{66} + \dots + g_{87}); C_1 = \frac{B Sc}{i n C}; \\
 g_6 &= B g_1 \text{Pr} - G r g_4; g_7 = B g_2 Sc - G s g_5; g_8 = -\omega; g_9 = \frac{g_6}{\text{Pr}^2 - \text{Pr} - \omega}; g_{10} = \frac{g_7}{Sc^2 - Sc - \omega}; g_{11} = \frac{-g_8}{\omega}; \\
 g_{12} &= \frac{G r g_4}{m_4^2 - m_4 - \omega}; g_{15} = \frac{\lambda}{k}; g_{13} = \frac{G s g_5}{m_6^2 - m_6 - \omega}; g_{14} = -(g_9 + \dots + g_{13}); g_{16} = -g_1^2 \text{Pr}^3 + \sigma g_1^2; \\
 g_{17} &= -g_2^2 \text{Pr } Sc^2 + \sigma g_2^2; g_{18} = -g_3^2 \text{Pr } m_2^2 + \sigma g_3^2; g_{19} = \sigma g_1; g_{20} = \sigma g_2; g_{21} = \sigma g_3; \\
 g_{22} &= -2 g_1 g_2 \text{Pr}^2 Sc + \sigma g_1 g_2; g_{23} = g_2 g_3 (\sigma - 2\text{Pr } Sc m_2); g_{24} = (\sigma - 2\text{Pr}^2 m_2) g_1 g_3; \\
 g_{44} &= -2 g_{11} \text{Pr } \sigma; g_{45} = -2 g_{11} g_3 \text{Pr } \sigma + B g_{29} m \text{Pr}; g_{46} = -2 g_{12} \text{Pr } \sigma; g_{47} = -2 g_{13} \text{Pr } \sigma; g_{48} = -2 g_{14} \text{Pr } \sigma; \\
 g_{49} &= 2B g_{27} m_2 \text{Pr}; g_{50} = -2 g_{12} g_3 \text{Pr}(\sigma + m_2 m_4); g_{51} = -2 g_{13} g_3 \text{Pr}(\sigma + m_2 m_6); \\
 g_{52} &= -2 g_{14} g_3 \text{Pr}(\sigma + m_2 m_8); g_{54} = -2 g_1 g_{12} \text{Pr}(\sigma + m_4 \text{Pr}); g_{53} = B g_{32} \text{Pr}(m_2 + \text{Pr}) - 2 g_3 g_9 \text{Pr}(\sigma + m_2 \text{Pr}); \\
 g_{55} &= -2 g_1 g_{13} \text{Pr}(\sigma + m_6 \text{Pr}); g_{56} = -2 g_1 g_{14} \text{Pr}(\sigma + m_8 \text{Pr}); g_{57} = -2\text{Pr}(g_1 g_{11} + g_9) \sigma + B g_{33} \text{Pr}^2; \\
 g_{58} &= -2 g_1 g_9 \text{Pr}(\sigma + \text{Pr}^2) + 2B g_{25} \text{Pr}^2; g_{59} = -2\sigma \text{Pr}(g_2 g_{11} + g_{10}) + B g_{28} \text{Pr } Sc; \\
 g_{62} &= -2 g_2 g_{12} \text{Pr}(\sigma + m_4 Sc); g_{60} = 2(g_1 g_{10} + g_2 g_9) \text{Pr}(\text{Pr } Sc - \sigma) + B g_{30} \text{Pr}(\text{Pr} + Sc); \\
 g_{63} &= -2 g_2 g_{13} \text{Pr}(\sigma + m_6 Sc); g_{61} = -2 g_3 g_{10} \text{Pr}(\sigma + Sc m_2) + B g_{31} \text{Pr}(m_2 + Sc); \\
 g_{64} &= -2 g_2 g_{14} \text{Pr}(\sigma + m_8 Sc); g_{65} = -2 g_2 g_{10} \text{Pr}(\sigma + Sc) + 2B g_{26} \text{Pr } Sc; \\
 g_{68} &= \frac{g_{46}}{m_4^2 - \text{Pr } m_4 - i n \text{Pr}}; g_{90} = -G r g_{66}; g_{91} = B g_{43} m_2 - G r g_{67}; g_{92} = -G r g_{89}; g_{93} = -G r g_{69}; g_{94} = -G r g_{70}; \\
 g_{95} &= 2B g_{37} m_2 - G r g_{71}; g_{96} = -G r g_{72}; g_{97} = -G r g_{73}; g_{98} = -G r g_{74}; f_1 = -G r g_{76}; \\
 g_{99} &= B g_{42} (\text{Pr} + m_2) - G r g_{75}; f_2 = -G r g_{77}; f_3 = -G r g_{78}; f_4 = B g_{34} \text{Pr} - G r g_{79}; f_5 = 2B g_{35} \text{Pr} - G r g_{80}; \\
 f_6 &= B g_{38} Sc - G r g_{81}; f_7 = B g_{40} (\text{Pr} + Sc) - G r g_{82}; f_9 = -G r g_{84}; f_8 = B g_{41} (m_2 + Sc) - G r g_{83}; \\
 f_{10} &= -G r g_{85}; f_{11} = -G r g_{86}; f_{12} = 2B g_{36} Ps - G r g_{87}; \omega = i n + \sigma;
 \end{aligned}$$

## Funding

This research received no external funding.

## Acknowledgments

The authors would like to thank the anonymous reviewers for their valuable comments and suggestions to improve the quality of the paper.

## Conflicts of Interest

The authors declare no conflict of interest.

## References

1. Pop and Ingham, D.B. Convective heat transfer: Mathematical and computational modelling of viscous fluids and porous media. *Pergamon, Oxford* **2001**.
2. Nield, D.A.; Bejan, A. Convection in porous media. *Springer, New York* **2013**.
3. Jean, L.A.; Claude, B.; Christian, G. Incompressible Newtonian fluid flow through a rigid porous medium. *Wiley Online Library* **2009**, <https://doi.org/10.1002/9780470612033.ch7>.
4. Devakar, M.; Ramgopal, N. Fully developed flows of two immiscible couple stress and Newtonian fluids through nonporous and porous medium in a horizontal cylinder. *Journal of Porous Media* **2015**, *18*, 549-558, <https://doi.org/10.1615/jpormedia.v18.i5.70>.
5. B. Veera Sankar, B. Rama Bhupal Reddy, Unsteady flow of Newtonian fluid through porous medium in two vertical cylinders with an inclined magnetic field. *Journal of Computer and Mathematical Sciences* **2019**, *10*, 361-374, <https://doi.org/10.29055/jcms/1015>.
6. Malleswari, K.; Sarojamma, G.; Sreelakshmi, K.; Vijayalakshmi, R.; Satya Narayana, P.V.; Vajravelu, K. Coupled effect of multi-slips and activation energy in a micropolar nanoliquid on a convectively heated elongated surface. *Heat Transfer* **2021**, *50*, 6237- 6258, <https://doi.org/10.1002/htj.22170>.
7. Satya Narayana, P.V.; Tarakaramu, N.; Harish Babu, D. Influence of chemical reaction on MHD couple stress nanoliquid flow over a bidirectional stretched sheet. *International Journal of Ambient Energy* **2021**, 1-11, <https://doi.org/10.1080/01430750.2021.1923569>.
8. Murthy, P.V.S.N.; Sutradhar, A.; Reddy, C.H.R. Double diffusive free convection flow past an inclined plate embedded in a non-Darcy porous medium saturated with a nanofluid. *Transport in Porous Media* **2013**, *9*, 553-564, <https://doi.org/10.1007/s11242-013-0160-z>.
9. Chamkha, A.J. Unsteady MHD convective heat and mass transfer past a semi-infinite vertical permeable moving plate with heat absorption. *International Journal of Engineering Science* **2014**, *42*, 217-230, [https://doi.org/10.1016/S0020-7225\(03\)00285-4](https://doi.org/10.1016/S0020-7225(03)00285-4).
10. Mamou, M.; Vasseur, P.; Bilgen, E.; Gobin, D. Double diffusive convection in an inclined slot filled with porous medium. *Journal of Mechanics in Fluids* **1995**, *14*, 629-652.
11. Kumari, M.; and Nath, G. Double diffusive unsteady mixed convection flow over a vertical plate embedded in a porous media. *International Journal of Energy Resources* **1989**, *13*, 419-430, <https://doi.org/10.1002/er.4440130406>.
12. Patil, P.M.; Roy, S.; Chamkha, A.J. Double diffusive mixed convection flow over a moving vertical plate in the presence of internal heat generation and chemical reaction. *Turkish Journal of Engineering Sciences* **2009**, *33*, 193-205, <https://doi.org/10.3906/muh-0905-21>.
13. Mallikarjuna, B.; and Bhuvanavijaya, R. Double diffusive convection of a rotating fluid over a vertical plate embedded in Darcy-Forchheimer porous medium with non-uniform heat sources. *International Journal of Emerging Trends in Engineering and Development* **2013**, *2*, 2249-6149.
14. Suresh Babu, R.; Rushi Kumar, B.; Dinesh P.A. Effects of variable fluid properties on a double diffusive mixed convection viscous fluid over a semi-infinite vertical surface in a sparsely packed medium. *Frontiers Heat and Mass Transfer* **2018**, *10*, <https://doi.org/10.5098/hmt.10.3>.
15. Harish Babu, D.; Samantha K.S.; Satya Narayana, P.V. Chemical reaction and thermophoresis effects on MHD mixed convection flow over an inclined porous plate with variable suction. *Advances in Fluid Dynamics* **2021**, 723-735, <https://doi.org/10.1007/978-981-15-4308-156>.
16. Pathak, G; Chaudhary, Maheshwari and Gupta, S.P. Effect of radiation on unsteady free convection flow bounded by an oscillatory plate with variable wall temperature. *International Journal of Applied Mechanics and Engineering* **2006**, *11*, 371. <https://doi.org/10.22457/apam.v16n2a23>.
17. Suresh Babu, R.; Rushi Kumar, B. A non-linear study of fluctuating fluid flow on MHD mixed convection through a vertical permeable plate. *Materials Science and Engineering* **2017**, *263*, 062029, <https://doi.org/10.1088/1757-899X/263/6/062029>.
18. Mohammad, A.Z. MHD heat and mass transfer of an oscillatory flow over a vertical permeable plate in a porous medium with chemical reaction. *Modern Mechanical Engineering* **2018**, *8*, 179-191, <https://doi.org/10.4236/mme.2018.83012>.
19. Rangasamy, P.; Murugesan, N. Soret and hall effect on unsteady free convection flow past an infinite vertical



- plate with oscillatory suction velocity and variable permeability. *International Journal of Heat and Technology* **2018**, 36, 808-816, <https://doi.org/10.18280/ijht.360305>.
20. Begum, A.S.; Nithya devi, N.; Öztö, H.F.; Hamdeh, N.A. Effects of variable temperature on mixed convection of a Cu-water nanofluid in a double-lid-driven porous enclosure with active middle vertical wall. *Journal of Porous Media* **2019**, 22, 48-497, <https://doi.org/10.1615/jpormedia.2019028911>.
  21. Venkateswarlu, B.; Bhagya Lakshmi, K.; Samantha K.S.; Satya Narayana, P.V. Magnetohydrodynamic oscillatory flow of a physiological fluid in an irregular channel. *SN Applied Sciences* **2019**, 1, 75-91, <https://doi.org/10.1007/s42452-019-1250-5>.
  22. Selimefendigil, F.; Öztö, H.F. Effects of local curvature and magnetic field on forced convection in a layered partly porous channel with area expansion. *International Journal of Mechanical Sciences* **2020**, 179, 105696, <https://doi.org/10.1016/j.ijmecsci.2020.105696>.
  23. Swarnalathamma, A.J.; Praveen Babu, D.M.; Veera Krishna, M. Time dependent permeability, Oscillatory suction and Hall effects on MHD Free convective flow through Porous medium over an infinite vertical plate. *Journal of Xidian University* **2020**, 14, 2009-2032, <https://doi.org/10.37896/jxu14.4/226>.
  24. Makhalemele, C.R.; Rundora, L.; Adesanya, S.O. Mixed convective flow of unsteady hydromagnetic couple stress fluid through a vertical channel filled with porous medium. *International Journal of Applied Mechanics and Engineering* **2020**, 25, 148-161, <https://doi.org/10.2478/ijame-2020-0055>.
  25. Pratibha, M.; Sweta, T. Effect of non-uniform heat source and radiation on unsteady MHD free convection flow past an infinite heated vertical plate in porous medium. *E-Jurnal Matematika* **2020**, 9, 219-230, <https://doi.org/10.24843/mtk.2020.v09.i04.p302>.
  26. Kamran, M.; Narahari, M.; Jaafar, A. Free convection flow past an impulsively started infinite vertical porous plate with Newtonian heating in the presence of heat generation and viscous dissipation. *AIP Conference Proceedings* **2014**, 1621, <https://doi.org/10.1063/1.4898461>.
  27. Das, S.; Mandal, C.; Jana, R. N. Radiation effects on unsteady free convection flow past a vertical plate with Newtonian heating. *International Journal of Computer Applications* **2012**, 41, 36-41, <https://doi.org/10.5120/5605-7864>.
  28. Rajesh, V.; Ali J. Chamkha. Unsteady convective flow past an exponentially accelerated infinite vertical porous plate with Newtonian heating and viscous dissipation. *International Journal of Numerical Methods for Heat & Fluid Flow* **2014**, 24, 1109-1123, <https://doi.org/10.1108/hff-05-2012-0122>.
  29. Venkateswarlu, B.; Satya Narayana, P.V.; Tarakaramu, N. Melting and viscous dissipation effects on MHD flow over a moving surface with constant heat source. *Transactions of A. Razmadze Mathematical Institute* **2019**, 172, 619-630, <https://doi.org/10.1016/j.trmi.2018.03.007>.
  30. Agarwal, S.P.; Anil Kumar. Effect of viscous dissipation on MHD unsteady flow through vertical porous medium with constant suction. *Advances in Mathematics: Scientific Journal* **2020**, 9, 7065-7073, <https://doi.org/10.37418/amsj.9.9.56>.
  31. Roy, K.; Ponalagusamy, R.; Murthy, P.V.S.N. The effects of double-diffusion and viscous dissipation on the oscillatory convection in a viscoelastic fluid saturated porous layer. *Physics of Fluids* **2020**, 32, 094108, <https://doi.org/10.1063/5.0020076>.
  32. Dipak, B.; Srinivasacharya, D. The variable gravity field and viscous dissipation effects on the convective instability in a porous layer with through flow: Brinkman model. *Journal of Porous Media* **2021**, 24, 1-13, <https://doi.org/10.1615/jpormedia.2021036098>.
  33. Ganesh, S.; Delhi Babu, R.; Karunakaran, K.C. Analysis of unsteady two dimensional MHD flow between two parallel plates under angular velocity with one plate moving uniformly and the other plate at rest and uniform suction at the stationary plate. *International Journal of Ambient Energy* **2020**, 1-7, <https://doi.org/10.1080/01430750.2020.1736626>.
  34. Jiang-Tao, H.; Shuo-Jun, M. Unsteady double diffusive convection inside a partial porous building enclosure subjected to time-periodic temperature boundary condition. *International Communications in Heat and Mass Transfer* **2021**, 122, 105128, <https://doi.org/10.1016/j.icheatmasstransfer.2021.105128>.
  35. Lazarus, R. Unsteady Magnetohydrodynamic mixed convective flow of a reactive casson fluid in a vertical channel filled with a porous medium. *Defect and Diffusion Forum* **2021**, 408, 33-49, <https://doi.org/10.4028/www.scientific.net/ddf.408.33>.
  36. Mahanta, M.; Sinha, S. Free convective MHD flow past a vertical plate through a porous medium with ramped wall temperature and concentration. *Journal of Mathematical and Computational Science* **2021**, 11, 23-41, <https://doi.org/10.28919/jmcs/5298>.
  37. Narsimlu, G.; Sudhakar Rao, T. Finite element solution of mass transfer effects on unsteady hydromagnetic convective flow past a vertical porous plate in a porous medium with heat source. *Journal of Mathematical and Computational Science* **2021**, 11, 5682-5702, <https://doi.org/10.28919/jmcs/6098>.
  38. Krishna, M.V.; Gangadhar Reddy, M.; Chamkha, A.J. Heat and mass transfer on unsteady MHD flow through an infinite oscillating vertical porous surface. *Journal of Porous Media* **2021**, 24, 81-100, <https://doi.org/10.1615/jpormedia.2020025021>.